CRYSTAL GROWTH & DESIGN

Communication

Cite This: *Cryst. Growth Des.* 2018, 18, 4849−4859

pubs.acs.org/crystal

Structural Isomerization of 2-Anilinonicotinic Acid Leads to a New Synthon in 6-Anilinonicotinic Acids

Siqing Peng,[†] Faquan Yu,[†] Danrui Xu,[†] Conggang Li,[‡] Sean R. Parkin,[§] Tonglei Li,[∥] Mingtao Zhang,*[,⊥] and Sihui Long*[,†]

[†]Key Laboratory for Green Chemical Process of Ministry of Education, School of Chemical Engineering and Pharmacy, Wuhan Institute of Technology, Wuhan, Hubei 430073, China

[‡]Wuhan Institute of Physics and Mathematics, Chinese Academy of Sciences, Wuhan, Hubei 430071, China

[§]Department of Chemistry, University of Kentucky, Lexington, Kentucky 40506, United States

[∥]Department of Industrial and Physical Pharmacy, Purdue University, West Lafayette, Indiana 47907, United States

[⊥]Department of Chemistry, Nankai University, Tianjin, 300071, China

Supporting Information

ABSTRACT: Through structural modification of 2-anilinonicotinic acid by isomerization, a new synthon, acid-aminopyridine, is created, and the two original synthons, i.e., the acid−acid homosynthon and acid−pyridine heterosynthon are no longer observed in the newly designed 6-anilinonicotinic acids. The new synthon has a hydrogen-bond strength rivaling that of the acid−acid homosynthon and the acid−pyridine heterosynthon, as suggested by theoretical calculations, which explains its formation.

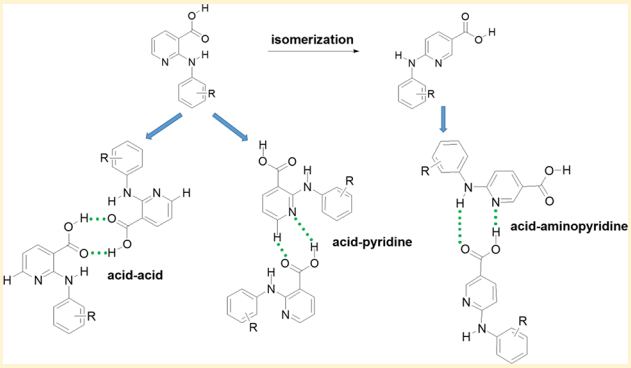

Anilinonicotinic acids, particularly 2-anilinonicotinic acids (2-ANAs), have been investigated as nonsteroidal anti-inflammatory drugs (NSAIDs), and clonixin and flunixin are two representatives.[1−3] 2-ANAs are conformationally flexible compounds with both carboxylic acid and pyridine groups, and they are known to form crystals sustained either on the acid−acid or acid−pyridine hydrogen-bonding motifs.[4−8] When the acid−acid dimer is observed, the molecules usually take a (near) coplanar conformation, and if the acid−pyridine heterosynthon is formed, a twisted conformation (i.e., the two aromatic rings are nonplanar) dominates.[4−6,9] Statistically, the acid−pyridine heterosynthon is preferred as it is energetically favored.[5,10−13] Yet, for 2-anilinonicotinic acids, either acid−acid or acid−pyridine synthon can be induced by crystal engineering approaches. To wit, the acid−acid homosynthon can be forced by installing highly electron-withdrawing groups such as fluorine on the benzene ring, and the acid−pyridine heterosynthon can be engineered either through introducing bulky (steric hindering) groups at the 2 and/or 6 position of the benzene ring or adding an alkyl group to the aniline N. In addition, a polymorphic form of 2-(phenyl-propyl-amino)-nicotinic acid (2-PPNA) was found to possess both the acid−acid homosynthon and acid−pyridine heterosynthon and the underlying mechanism was explored which demonstrates the subtle interplay between conformation and intra/intermolecular interactions (Figure 1).[14−24]

In the aforementioned 2-ANA compounds, delocalization of the lone pair electrons on the anilino N renders the C−N bond (shown in 1a) partially double, which means the molecules can have either E or Z configuration, theoretically.[25−27] In practice, only the Z-isomer is observed in the diarylamine compounds due to the formation of an intramolecular hydrogen bond between NH and the carbonyl C═O of the carboxylic acid.[28−32] For the alkylated anilino diarylamines such as 2-PPNA, the molecules are E-isomers instead, likely due to steric hindrance.[33,34]

2-ANAs are not the only compounds with both carboxylic acid and pyridine functionalities. What would happen if the structural variation is based on shifting the whole benzene ring from position 2 of the pyridine ring to position 6, i.e., isomerization is utilized to modify the molecules?[35−37] These new compounds, i.e., 6-anilinonicotinic acids (6-ANAs), have not been investigated either in medicinal chemistry or in crystal engineering. Structurally, they still possess partial double bond property for the corresponding C−N bond (Figure 2a), which should again lead to E and Z configurational isomers, and the intramolecular hydrogen bond between

Received: June 2, 2018
Revised: July 27, 2018
Published: August 3, 2018

DOI: 10.1021/acs.cgd.8b00840
Cryst. Growth Des. 2018, 18, 4849−4859

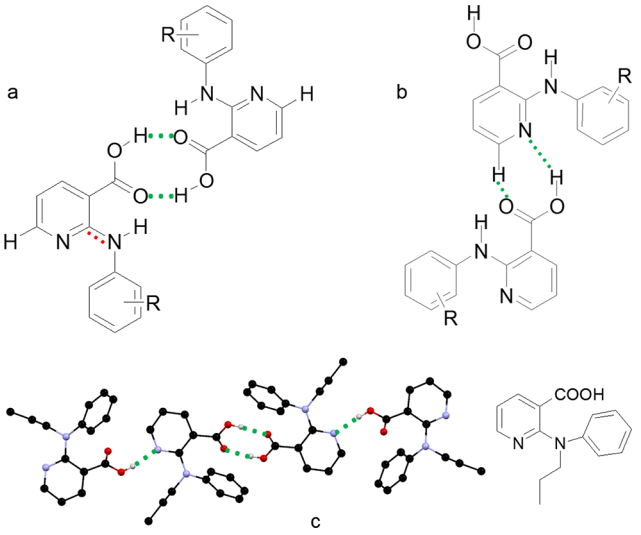

Figure 1. Acid−acid homosynthon (a), acid−pyridine heterosynthon (b), and coexistence of both synthons in 2-PPNA (c).

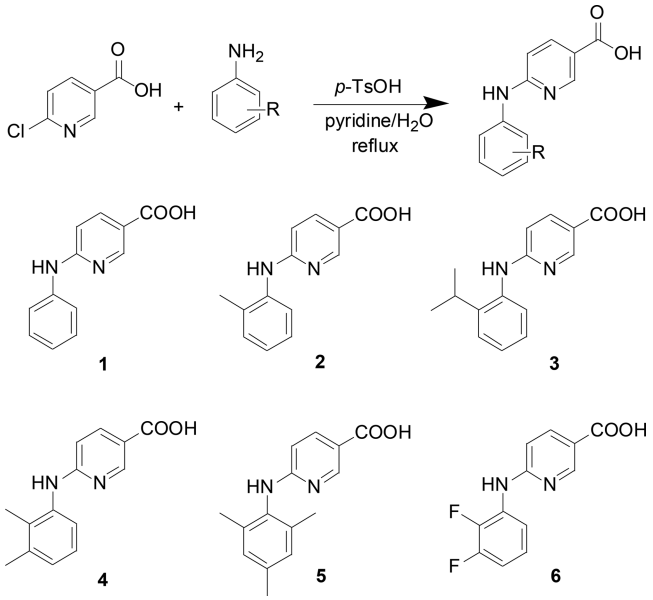

Figure 3. Synthesis of six 6-ANAs.

NH and C═O is no longer feasible. Will the acid−acid homosynthon (2a) be preferred or the acid−pyridine heterosynthon (2c) be favored, or will new synthons such as the acid−aminopyridine (2d) and the aminopyridine−aminopyridine (2b) emerge in the newly designed 6-ANAs[38−42] (Figure 2)? Investigation of 6-ANAs should shed light on the relationship between the location of functional groups and/or conformation and crystal packing (e.g., polymorphism) and also contribute to the field of crystal structure prediction.[43−46]

In this study, we designed a series of 6-ANAs and investigated the effect of isomerization on the crystal structure, particularly on the synthon formation.

Six 6-ANAs were synthesized according to a similar approach to the synthesis of 2-anilinonicotinic acid, i.e., the SNAr reaction (Figure 3).[47,48] (the detailed procedure and characterization are included in the Supporting Information)

A preliminary polymorph screening was carried out for each compound.[49−51] These compounds are not particularly soluble in most common solvents used for crystal growth. For all the compounds, one crystal form has been discovered so far. All the crystals are colorless with various morphologies. The crystal structures were determined by single-crystal X-ray diffraction. Crystals of compound **4** were triclinic, space group $P\bar{1}$, while all the other compounds gave orthorhombic crystals with varying space groups. Crystallographic data are given in Table 1. For complete CIF files, see the Supporting Information. All the crystals have only one crystallographically independent molecules ($Z' = 1$) in each of the asymmetric units except for that of compound **4**, which has two independent molecules ($Z' = 2$). The benzene ring of the molecule in compound **6** is disordered over two positions with the major one having an occupancy of 92%. All molecules

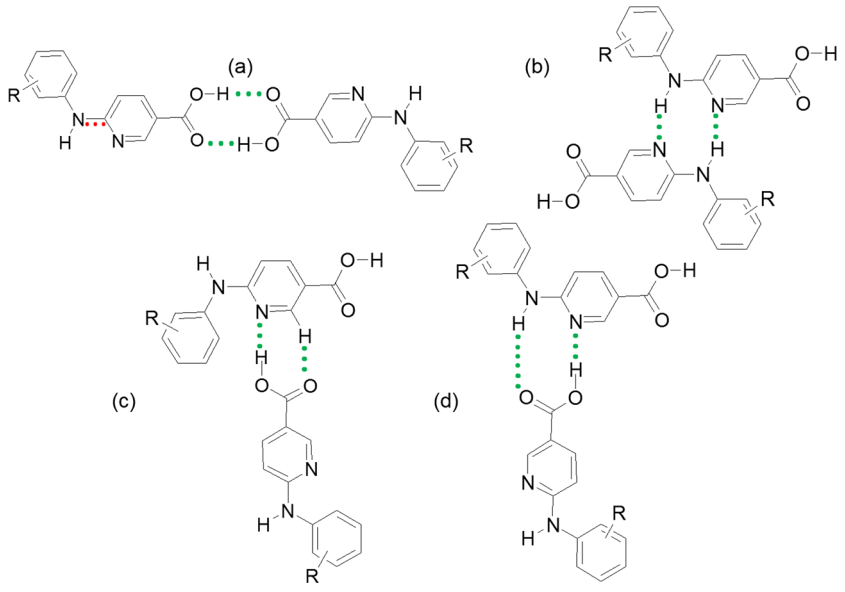

Figure 2. Possible synthons in the 6-ANA crystals: a. acid−acid homosynthon, b. aminopyridine−aminopyridine homosynthon, c. acid−pyridine heterosynthon, d. acid−aminopyridine heterosynthon.

DOI: 10.1021/acs.cgd.8b00840
Cryst. Growth Des. 2018, 18, 4849−4859

Table 1. Crystallographic Data of Compounds 1−6

	1	2	3	4	5	6
formula	$C_{12}H_{10}N_2O_2$	$C_{13}H_{12}N_2O_2$	$C_{15}H_{16}N_2O_2$	$C_{14}H_{14}N_2O_2$	$C_{15}H_{16}N_2\ O_2$	$C_{12}H_8F_2N_2O_2$
formula weight	214.22	228.25	256.30	242.27	256.30	250.20
crystal size (mm)	0.15 × 0.15 × 0.03	0.30 × 0.10 × 0.10	0.50 × 0.40 × 0.05	0.4 × 0.3 × 0.1	0.30 × 0.20 × 0.05	0.20 × 0.10 × 0.10
crystal system	orthorhombic	orthorhombic	orthorhombic	triclinic	orthorhombic	orthorhombic
space group	*Pbca*	*Pbca*	*Pca*21	$P\bar{1}$	*Pbca*	*Pca*21
a/Å	13.8359(2)	13.7049(3)	28.3815(12)	10.7437(4)	6.47500(10)	19.57220(10)
b/Å	7.1891(4)	7.6401(2)	5.3804(2)	10.8657(4)	13.6795(3)	3.9750(4)
c/Å	20.9809(6)	21.0500(5)	8.5880(4)	11.3689(5)	29.3965(8)	13.5879(6)
α/°	90.00	90.00	90.00	101.8235(16)	90.00	90.00
β/°	90.00	90.00	90.00	101.4872(17)	90.00	90.00
γ/°	90.00	90.00	90.00	100.7778(16)	90.00	90.00
Z, *Z*′	8, 1	8, 1	4, 1	4, 2	8, 1	4, 1
V/Å^3	2086.92(13)	2204.08(9)	1311.42(10)	1236.58(8)	2603.79(10)	1057.13(12)
D_{cal}/g × cm^{-3}	1.364	1.376	1.298	1.301	1.308	1.572
T/K	90(2)	90(2)	90(2)	90(2)	90(2)	90(2)
abs coeff (mm^{-1})	0.095	0.095	0.087	0.089	0.088	0.133
F(000)	896	960	544	512	1088	512
q range(deg)	1.94	1.93	1.43	1.89	2.77	2.56
	23.81	27.45	27.47	27.23	27.50	27.45
limiting indices	$-15 \le h \le 15$	$-9 \le h \le 9$	$-36 \le h \le 36$	$-13 \le h \le 13$	$-8 \le h \le 8$	$-24 \le h \le 24$
	$-8 \le k \le 8$	$-17 \le k \le 17$	$-6 \le k \le 6$	$-13 \le k \le 13$	$-17 \le k \le 17$	$-5 \le k \le 5$
	$-23 \le l \le 23$	$-27 \le l \le 27$	$-11 \le l \le 11$	$-14 \le l \le 14$	$-37 \le l \le 38$	$-17 \le l \le 17$
completeness to 2*θ*	100.0%	100.0%	99.8%	99.1%	99.9%	100.0%
Unique reflections	1891	1689	1795	3803	6248	921
$R_1[I > 2\sigma(I)]$	0.0495	0.0481	0.0440	0.0492	0.0556	0.0519
wR_2 (all data)	0.1420	0.1375	0.1282	0.1385	0.1588	0.1481

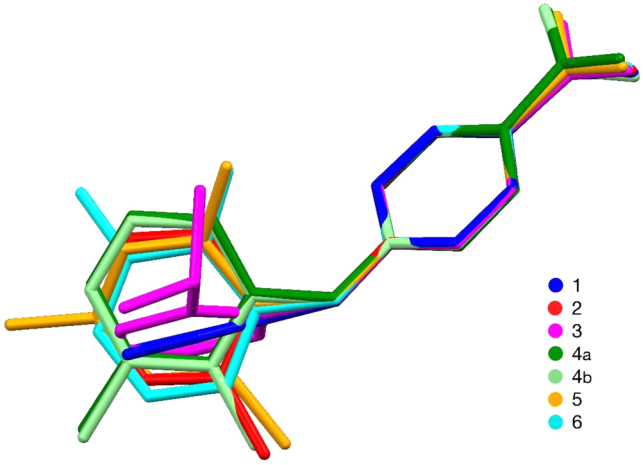

Figure 4. Superposition of seven crystallographically independent molecules in the six crystal structures.

Table 2. Hydrogen Bond Parameters of OH···N and NH···O in Five 6-ANA Compounds

	1	2	3	5	6
OH···N bond length (Å)	1.801	1.795	1.864	1.816	1.769
OH···N bond angle (deg)	167.91	168.86	175.38	174.12	168.32
NH···O bond length (Å)	2.018	2.092	1.912	1.944	1.981
NH···O bond angle (deg)	176.39	171.78	175.88	172.53	176.77

adopt the E configuration. The molecules have dihedral angles in the range from 40° to 60° (compound **1**: 45.14 (8)°; compound **2**: 42.22 (5)°; compound **3**: 61.25 (10)°; compound **4**: A, 50.70(6)° and B, 50.57(6)°; compound **5**: 61.19 (7)°; compound **6**: 43.07 (14)°).

Conformational variability is readily apparent in a superposition of all seven experimental conformations (Figure 4).

Neither the conventional acid−acid homosynthon nor the acid−pyridine heterosynthon was observed in the crystal structures. Instead, an intermolecular hydrogen bond between the carboxylic acid of one molecule and the pyridine N and amino NH of another molecule, namely an acid-aminopyridine heterosynthon, was formed ($R_2^2(8)$[52−54]). In a sense, this new synthon is an enhanced version of the previous acid−pyridine heterosynthon, because in the acid−pyridine heterosynthon, the sp^2 C−H adjacent to the pyridine N also hydrogen bonds with the carbonyl O of the carboxylic acid.

Aside from compound **4**, the aforementioned twisted molecules form one-dimensional chains based on the acid-aminopyridine heterosynthon (Figures 5−9), with varying hydrogen bond parameters (Table 2).

In compound **4**, the two molecules (**I-A** and **I-B**) in the asymmetric unit have nearly identical dihedral angles of 50.70(6)° and 50.57(6)° between the two aromatic rings. The molecules form one-dimensional chains sustained on a heterogeneous hydrogen-bonded dimer ($R_2^2(8)$) between the carboxylic acid of one conformer and the pyridine N and secondary amine of the other conformer (Figure 10). The hydrogen bond between the carboxylic acid OH of conformer B and pyridine N of conformer A has a bond length of 1.815 Å and bond angle of 169.32°; the corresponding hydrogen bond between the carboxylic acid OH of conformer A and pyridine N of conformer B has parameters of 1.840 Å and 171.34°. Meanwhile, the hydrogen bond between the secondary NH of conformer A and the carbonyl O of conformer B has

DOI: 10.1021/acs.cgd.8b00840
Cryst. Growth Des. 2018, 18, 4849−4859

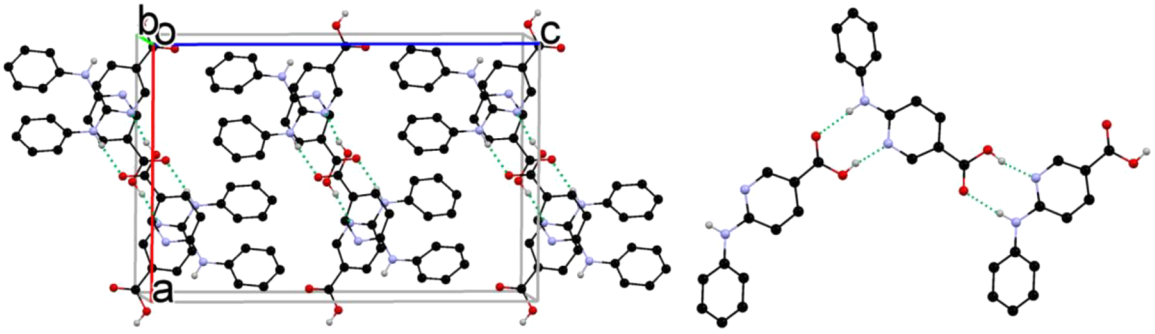

Figure 5. Crystal packing of compound **1**. For clarity, only intermolecular hydrogen bonds are shown (dotted line).

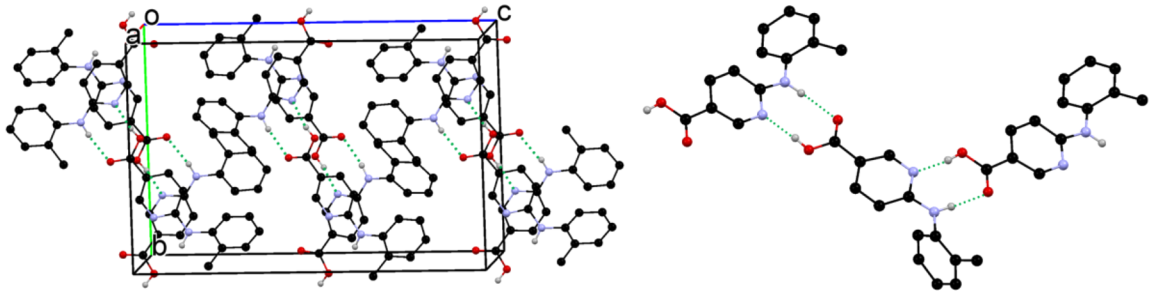

Figure 6. Crystal packing of compound **2**. For clarity, only intermolecular hydrogen bonds are shown (dotted line).

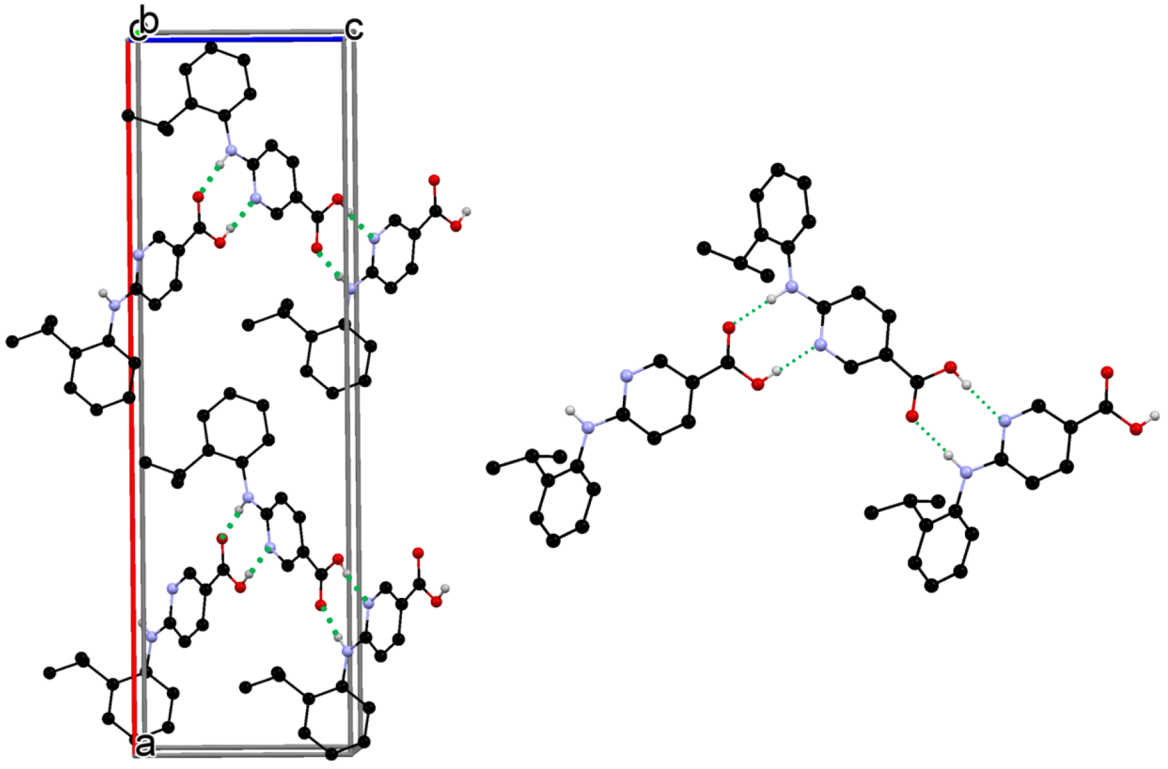

Figure 7. Crystal packing of compound **3**. For clarity, only intermolecular hydrogen bonds are shown (dotted line).

parameters of 2.019 Å and 169.88°, and the hydrogen bond between the secondary NH of conformer B and the carbonyl O of conformer A has almost identical parameters of 2.014 Å and 170.03°.

Since the molecules in all six crystals take a twisted conformation, we wondered about the energy difference between planar and twisted conformations. To that end, we considered compound **1** as an example. Due to the partial double bond property of C6−N7 (bond length 1.363 Å, while a typical C−N single bond has a bond length of 1.47 Å, and C═N has a bond length of 1.29 Å[55]), there are two configurational isomers of **1**, named **1**-Z and **1**-E, as shown in Figure 11. Single-molecule isomers of **1** and their hydrogen-bonded dimers were optimized from various initial conformations at the B3LYP/6-311+G(d,p)[56,57] and m06-2x[58]/Def2QZVP[59] level to identify possible stable conformations

DOI: 10.1021/acs.cgd.8b00840
Cryst. Growth Des. 2018, 18, 4849−4859

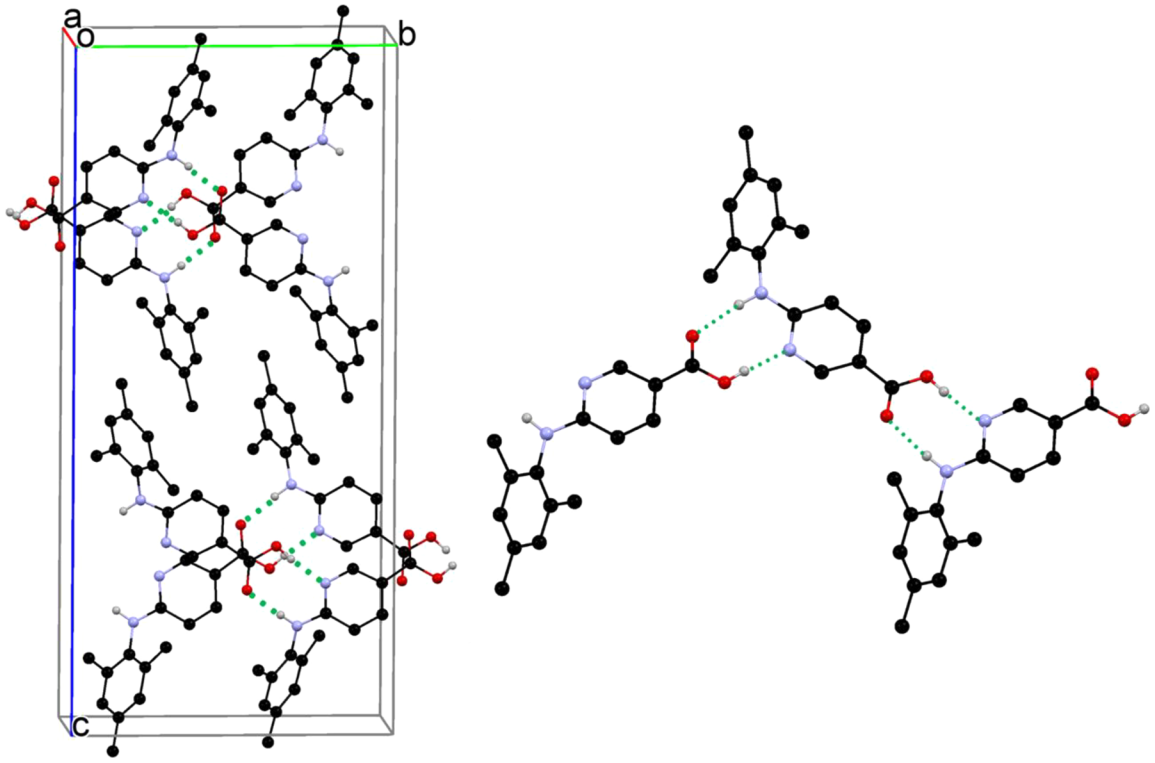

Figure 8. Crystal packing of compound **5**. For clarity, only intermolecular hydrogen bonds are shown (dotted line).

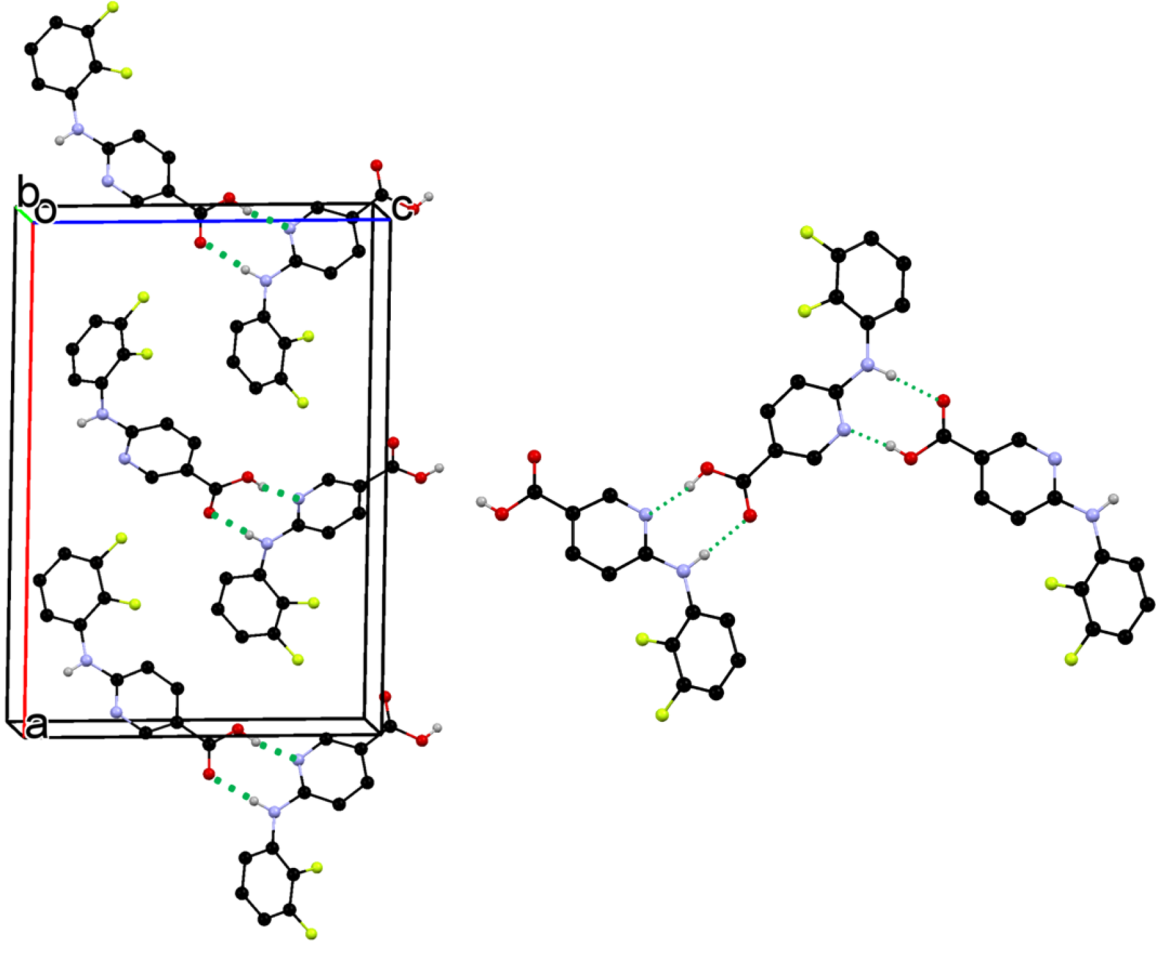

Figure 9. Crystal packing of compound **6**. For clarity, only intermolecular hydrogen bonds are shown (dotted line).

DOI: 10.1021/acs.cgd.8b00840
Cryst. Growth Des. 2018, 18, 4849−4859

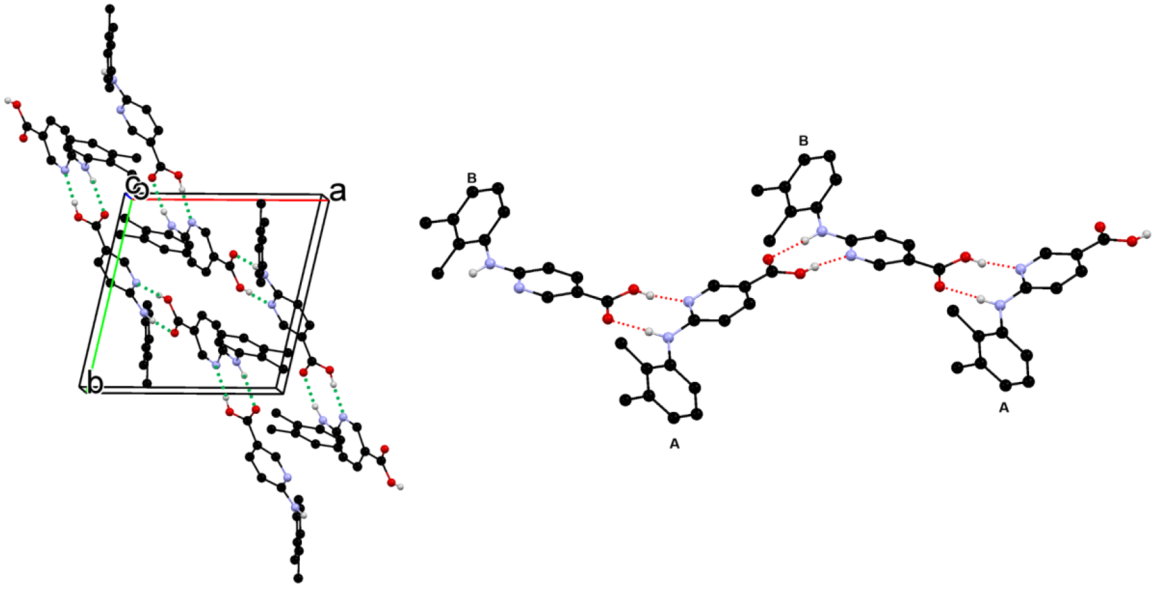

Figure 10. Crystal packing of compound **4**. For clarity, only intermolecular hydrogen bonds are shown (dotted line).

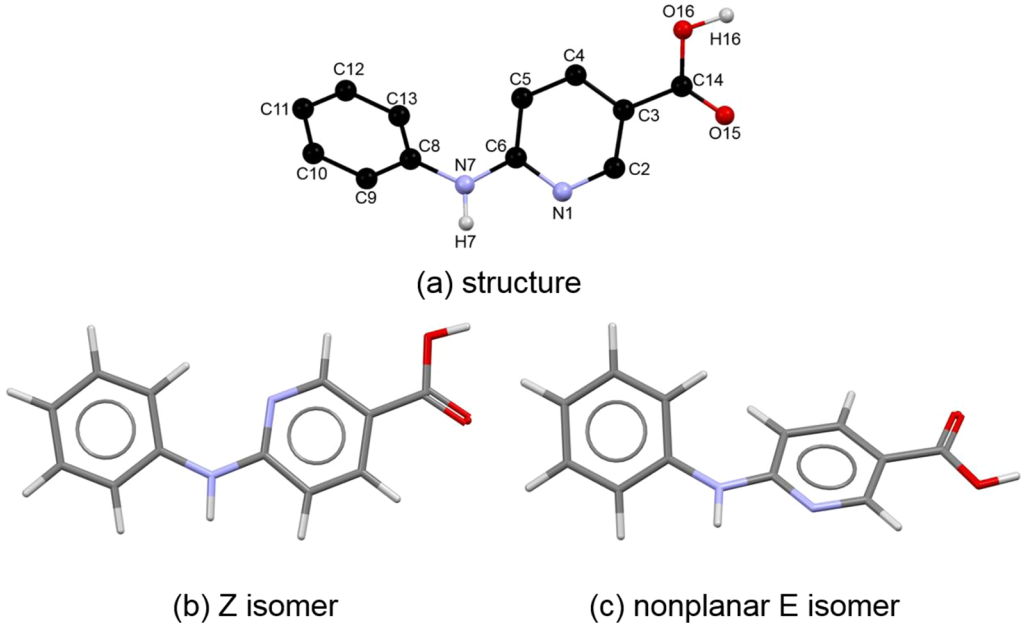

Figure 11. Structure of **1** from the crystal structure with atoms labeled (a); planar Z-isomer from optimization (b); nonplanar E-isomer from optimization (c).

(using Gaussian16, Gaussian, Inc., Wallingford, CT, USA).[60] Frequency calculations were performed for all optimized structures to identify energy minima (zero imaginary frequency, except for the hypothetical *Cs*-symmetry restricted E-isomer). Intermolecular interactions were then calculated with the basis set superposition error (BSSE) considered by the counterpoise method. Dispersion energies were evaluated using Grimme's DFT-D3 corrections with Becke–Johnson damping.[61,62] The temperature (298.15 K) and zero-point vibrational energies (ZPVE) were also considered. All calculations were conducted on a Linux cluster[63−65]

The optimized molecule of **1**-Z gives a planar structure owing to the delocalized conjugation of both the aromatic rings and the lone pair electrons of the secondary amine N atom. **1**-E, however, is twisted because of the repulsion between the H atom on the pyridine ring and the H atom on the benzene ring. This twisted conformation has a torsion angle of 44.6°, which is consistent with the torsion angle of 45.1° found in the conformer of the X-ray structure. A planar E-isomer with assumed *Cs* symmetry restriction gave an imaginary vibration frequency 3.06 kcal/mol higher in energy than that of the twisted **1**-E. The **1**-Z isomer is less than 1 kcal/mol higher in energy than that of the twisted **1**-E (0.63 or 0.72 kcal/mol of Gibbs free energy based on B3LYP/6-311+G(d,p) level or m06-2x/Def2QZVP level, respectively). The similar stability between **1**-Z and **1**-E indicates that both isomers could exist in the crystal synthons.

We then examined the free energies of these different possible synthons; their energies are listed in Table 3:

DOI: 10.1021/acs.cgd.8b00840
Cryst. Growth Des. 2018, 18, 4849−4859

Table 3. Calculated Free Energies of the Possible Synthons

synthon	BSSE (kcal/mol)	ΔG (kcal/mol)[a,c]	ΔG (kcal/mol)[b,c]
1-EE-I	0.77	−6.18	−5.94
1-EE-II	0.66	−1.01	−0.05
1-EE-III	0.88	−5.58	−3.95
1-EE-IV	1.05	−3.01	0.16
1-ZZ-II	1.34	0.67	0.93
1-ZZ-II*	1.56	1.08	1.12
1-EZ-III	0.90	−5.62	−3.97

[a]Energies calculated at B3LYP/6-311+g(d,p) level with Grimme's DFT-D3 correction with Becke−Johnson damping, BSSE correction, zero-point vibrational energies (ZPVE), and thermal correction considered. [b]Energies calculated at m06-2x/Def2QZVP level by single-point calculations with Grimme's DFT-D3 correction considered. BSSE correction was omitted. Zero-point vibrational energies and thermal correction come from the B3LYP/6-311+g(d,p) level. [c]The ΔG values are relative energies to their constituents, i.e., $\Delta G(EZ) = G(EZ) - G(E) - G(Z)$. A negative ΔG means the synthon is energetically favored.

Four synthons **1**-EE-I, **1**-EE-II, **1**-EE-III, and 1-EE-IV formed by **1**-E are shown in Figure 12. All four synthons are ring dimers by different hydrogen bond types, O−H···O in I, C−H···O and O−H···N in II, O−H···N in III, and N−H···N in IV. The calculated binding energies are −6.18 kcal/mol, −1.01 kcal/mol, −5.58 kcal/mol, and −3.01 kcal/mol, respectively. The C−H···O hydrogen bond in II is much weaker than O−H···O, N−H···N, and O−H···N, so the binding energy of II is correspondingly lower than that of I, III, and IV, while I and III show similar binding energies. The electronegativity of N in pyridine is less than that of O in the carboxyl, which makes carboxyl a better hydrogen bond acceptor, so the hydrogen bonds in 1-EE-I and 1-EE-III are stronger than that in 1-EE-IV. The corresponding free energies calculated at m06-2x/Def2QZVP level in general agree with those from the B3LYP/6-311+g(d,p) level with the only discrepancy observed for **1**-EE-IV, which deserves further investigation. Nevertheless, the comparison holds only for the dimers. For types II and III hydrogen bonding patterns, infinite chains are possible, which should provide additional stability. For example, when we consider four molecules, for type I dimer, two dimers will form, while for types II and III, three dimers become feasible, which should be more stable.

For Z-isomers of **1** to form a II-type synthon the molecule must twist to a larger degree to make the pyridine N atom accessible for hydrogen bonding; thus **1**-ZZ-II and **1**-ZZ-II*

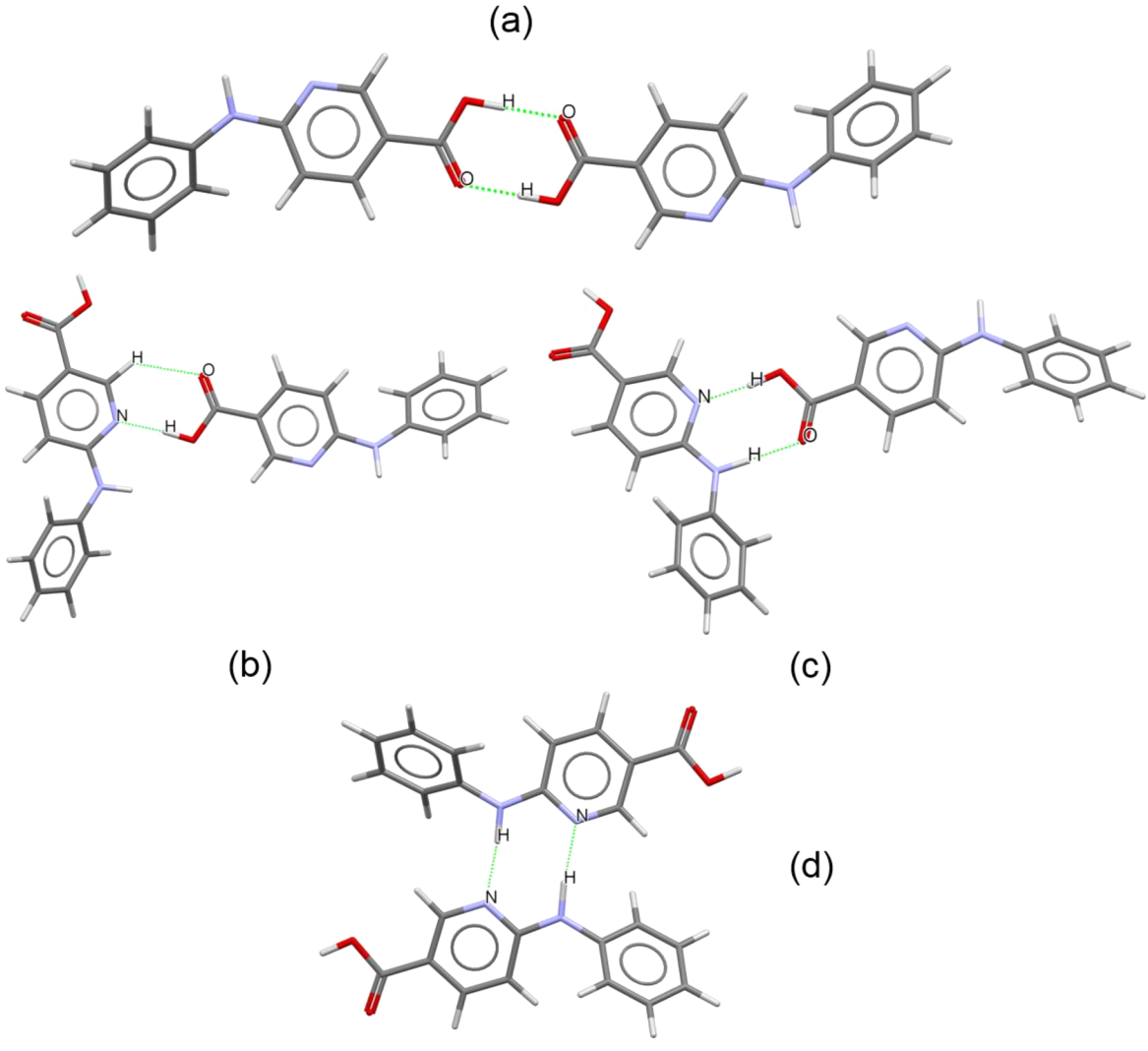

Figure 12. Structure of the synthons of (a) **1**-EE-I, (b) **1**-EE-II, (c) **1**-EE-III, and (d) 1-EE-IV.

DOI: 10.1021/acs.cgd.8b00840
Cryst. Growth Des. 2018, 18, 4849−4859

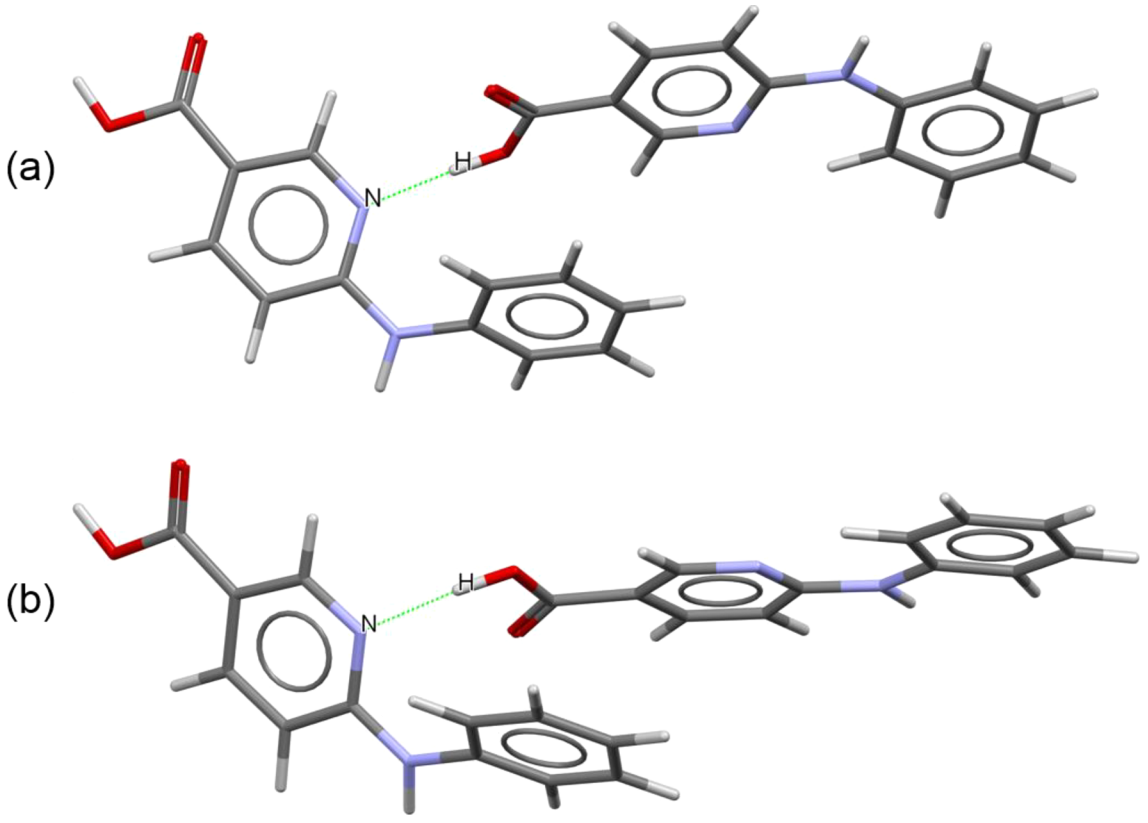

Figure 13. Structure of the synthons of **1**-ZZ-II (a) and **1**-ZZ-II* (b).

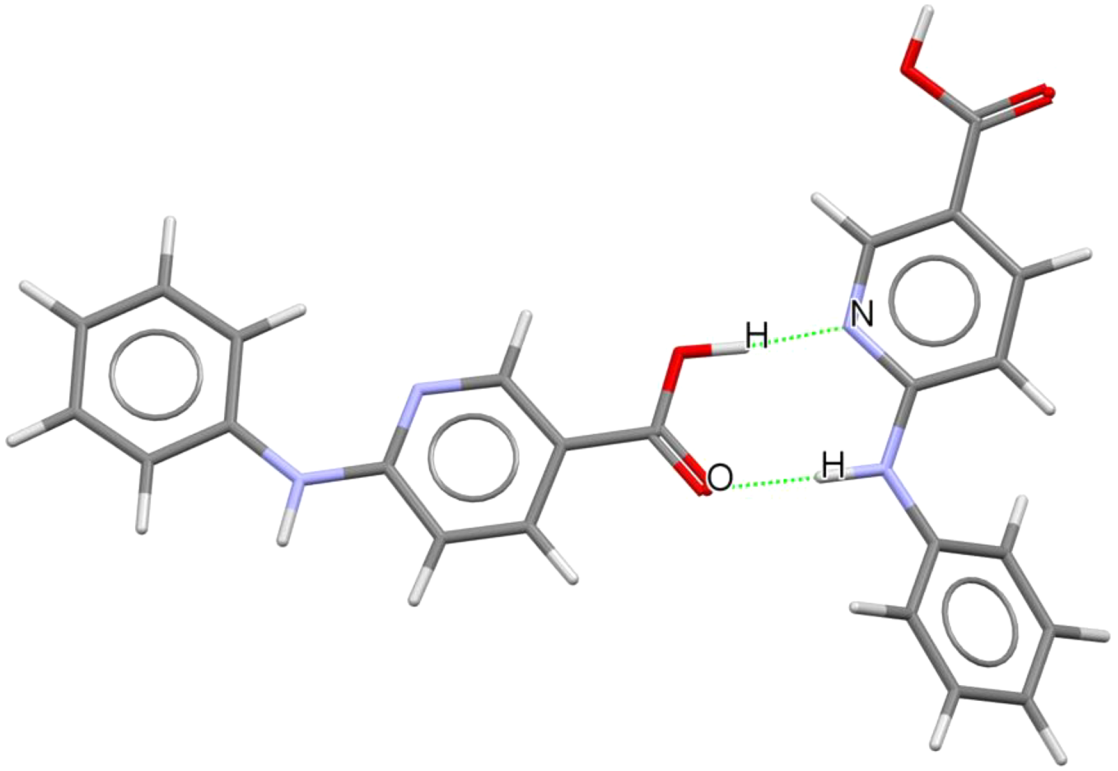

Figure 14. Structure of the synthons of **1**-EZ-III.

(Figure 13) were optimized with different twisted orientations. Their binding energies, at 0.67 and 1.08 kcal/mol, respectively, mean they are not thermodynamically favored. Moreover, a **1**-EZ-III (Figure 14) synthon formed by an E-isomer and a Z-isomer would have a binding energy of −5.62 kcal/mol, which is similar to that of **1**-EE-III or **1**-EE-I. These data suggest that likely the E/Z isomers compete with each other during the process of synthon utilization.

DOI: 10.1021/acs.cgd.8b00840
Cryst. Growth Des. 2018, 18, 4849−4859

In all six structures, the EE-III type synthon is observed which is in agreement with the stability analysis. Yet, the EZ-III type synthon could be a good alternate given the opportunity.

Synthons play an important role in crystal engineering. New synthons can be revealed either by chance or by design. In this paper, a new synthon was created through structural modification of 2-anilinonicotinic acids to 6-anilinonicotinic acids. The new synthon has a similar hydrogen-bond strength to that of the normally observed synthons in 2-anilinonicotinic acids, i.e., acid−acid homosynthon and acid−pyridine heterosynthon, which justifies its formation in the crystals.

■ ASSOCIATED CONTENT

Supporting Information

The Supporting Information is available free of charge on the ACS Publications website at DOI: 10.1021/acs.cgd.8b00840.

Atomic coordinates and energies for the optimized molecules (PDF)

Accession Codes

CCDC 1846851−1846853 and 1846855−1846857 contain the supplementary crystallographic data for this paper. These data can be obtained free of charge via www.ccdc.cam.ac.uk/data_request/cif, or by emailing data_request@ccdc.cam.ac.uk, or by contacting The Cambridge Crystallographic Data Centre, 12 Union Road, Cambridge CB2 1EZ, UK; fax: +44 1223 336033.

■ AUTHOR INFORMATION

Corresponding Authors

*Email: zhangmt@nankai.edu.cn.

*E-mail: sihuilong@wit.edu.cn; longsihui@yahoo.com. Phone: (86) 15549487318.

ORCID

Faquan Yu: 0000-0002-5062-8731

Conggang Li: 0000-0002-5798-1722

Tonglei Li: 0000-0003-2491-0263

Sihui Long: 0000-0002-4424-6374

Notes

The authors declare no competing financial interest.

■ ACKNOWLEDGMENTS

S.P. and S.L. thank Natural Science Foundation of Hubei Province (2014CFB787) and the President's Fund of Wuhan Institute of Technology (CX2016075) for financial support.

■ REFERENCES

(1) Sherlock, M. H.; Sperber, N. *Antinflammatory and analgesic pharmaceuticals containing nicotinic acid derivatives* Japanese Patent JP 51005386B, 1976.

(2) Sherlock, M. H. *N-Methyl-D-glucamine salt of 2-(2-methyl-3-trifluoromethylanilino)nicotinic acid in the treatment of pain*. U.S. Patent US 3891761A, 1975.

(3) Takasuka, M.; Nakai, H.; Shiro, M. Infrared Spectral and X-Ray Studies of Polymorphic Forms of *242*-Methyl-3-chloroanilino)n icotinic Acid. *J. Chem. Soc., Perkin Trans. 2* **1982**, *2*, 1061−1067.

(4) Long, S.; Li, T. Enforcing Molecule's π-Conjugation and Consequent Formation of the Acid-Acid Homosynthon over the acid−pyridine Heterosynthon in 2-Anilinonicotinic Acids. *Cryst. Growth Des.* **2010**, *10*, 2465−2469.

(5) Long, S.; Li, T. Controlled Formation of the acid−pyridine Heterosynthon over the Acid-Acid Homosynthon in 2-Anilinonicotinic Acids. *Cryst. Growth Des.* **2009**, *9*, 4993−4997.

(6) Long, S.; Parkin, S.; Siegler, M.; Brock, C. P.; Cammers, A.; Li, T. Polymorphism of an Organic System Effected by the Directionality of Hydrogen-Bonding Chains. *Cryst. Growth Des.* **2008**, *8*, 3137−3140.

(7) Chen, P.; Zhang, Z.; Parkin, S.; Zhou, P.; Cheng, K.; Li, C.; Yu, F.; Long, S. Preferred formation of the carboxylic acid−pyridine heterosynthon in 2-anilinonicotinic acids. *RSC Adv.* **2016**, *6*, 81101−81109.

(8) Mukherjee, A.; Desiraju, G. R. Combinatorial Exploration of the Structural Landscape of Acid−Pyridine Cocrystals. *Cryst. Growth Des.* **2014**, *14*, 1375−1385.

(9) Murthy, H. M. K.; Vijayan, M. 2-{[3-(Trifluoromethyl)phenyl]-amino}-3-pyridinecarbo xylic Acid* (Niflumic Acid). *Acta Crystallogr., Sect. B: Struct. Crystallogr. Cryst. Chem.* **1979**, *35*, 262−263.

(10) Steiner, T. Competition of hydrogen-bond acceptors for the strong carboxyl donor. *Acta Crystallogr., Sect. B: Struct. Sci.* **2001**, *57*, 103−106.

(11) Aakeröy, C. B.; Beatty, A. M.; Helfrich, B. A. Total Synthesis" Supramolecular Style:Design and Hydrogen-Bond-Directed Assembly of Ternary Supermolecules. *Angew. Chem., Int. Ed.* **2001**, *40*, 3240−3242.

(12) Shattock, T. R.; Arora, K. K.; Vishweshwar, P.; Zaworotko, M. J. Hierarchy of Supramolecular Synthons: Persistent Carboxylic Acid · · · Pyridine Hydrogen Bonds in Cocrystals That also Contain a Hydroxyl Moiety. *Cryst. Growth Des.* **2008**, *8*, 4533−4545.

(13) Vishweshwar, P.; Nangia, P.; Lynch, V. M. Molecular Complexes of Homologous Alkanedicarboxylic Acids with Isonicotinamide: X-ray Crystal Structures, Hydrogen Bond Synthons, and Melting Point Alternation. *Cryst. Growth Des.* **2003**, *3*, 783−790.

(14) Desiraju, G. R.; Parshall, G. W. Crystal Engineering. The Design of Organic Solid. *Materials Science Monographs A* **1989**, *54*, 312−326.

(15) Pepinsky, R. Crystal Engineering: A New Concept in Crystallography. *Phys. Rev.* **1955**, *100*, 971.

(16) Schmidt, G. M. J. Photodimerization in the Solid State. *Pure Appl. Chem.* **1971**, *27*, 647−678.

(17) Kitaigorodskii, A. I. *Molecular Crystals and Molecules*. Academic Press: New York, 1973.

(18) Braga, D.; Grepioni, F.; Desiraju, G. R. Crystal Engineering and Organometallic Architecture. *Chem. Rev.* **1998**, *98*, 1375−1405.

(19) Braga, D.; Grepioni, F.; Orpen, A. G., Eds. *Crystal Engineering. From Molecules and Crystals to Material*; Kluwer Academic Publishers, 1999; Vol. *538*.

(20) Desiraju, G. R., Eds. *Crystal Design. Structure and Function. Perspectives in Supramolecular Chemistry*; Wiley: Chichester, 2003.

(21) Tiekink, E. R.; Vittal, J. J., Eds. *Frontiers in Crystal Engineering*; Wiley: Chichester, 2005.

(22) Desiraju, G. R. Supramolecular Synthons in Crystal Engineering-A New Organic Synthesis. *Angew. Chem., Int. Ed. Engl.* **1995**, *34*, 2311−2327.

(23) Desiraju, G. R. Crystal Engineering: A Holistic View. *Angew. Chem., Int. Ed.* **2007**, *46*, 8342−8356.

(24) Dubey, R.; Desiraju, G. R. Combinatorial selection of molecular conformations and supramolecular synthons in quercetin cocrystal landscapes: a route to ternary solids. *IUCrJ* **2015**, *2*, 402−408.

(25) Krishnan, V. V.; Vazquez, S.; Maitra, K.; Maitra, S. Restricted amide rotation with steric hindrance induced multiple conformations. *Chem. Phys. Lett.* **2017**, *689*, 148−151.

(26) Krishnan, V. V.; Thompson, W. B.; Maitra, K.; Maitra, S. Modulations in restricted amide rotation by steric induced conformational trapping. *Chem. Phys. Lett.* **2012**, *523*, 124−127.

(27) Kleinpeter, E.; Koch, A. Identification of mesomeric substructures by through-space NMR shieldings (TSNMRS). Trimethine cyanine/merocyanine-like or aromatic p-electron delocalization? *Tetrahedron* **2017**, *73*, 4265−4274.

(28) Matsuhira, T.; Yamamoto, H.; Okamura, T.; Ueyama, N. Manipulation of an intramolecular NH···O hydrogen bond by photoswitching between stable E/Z isomers of the cinnamate framework. *Org. Biomol. Chem.* **2008**, *6*, 1926−1933.

DOI: 10.1021/acs.cgd.8b00840
Cryst. Growth Des. 2018, 18, 4849−4859

(29) Lewis, F. D.; Yoon, B. A.; Arai, T.; Iwasaki, T.; Tokumaru, K. Molecular Structure and Photochemistry of (E)- and (Z)-2-(2-(2-Pyridyl)ethenyl)indole. A Case of Hydrogen Bond Dependent One-way Photoisomerization. *J. Am. Chem. Soc.* **1995**, *117*, 3029−3036.
(30) Arai, T.; Moriyama, M.; Tokumaru, K. Novel Photoinduced Hydrogen Atom Transfer through Intramoleeular Hydrogen Bonding Coupled with Cis-Trans Isomerization in cis- 1 - (2-Pyrrolyl) −2- (2-quino1yl)ethene. *J. Am. Chem. Soc.* **1994**, *116*, 3171−3172.
(31) Ikegami, M.; Arai, T. Photoisomerization and Fluorescence Properties of Hemiindigo Compounds Having Intramolecular Hydrogen Bonding. *Bull. Chem. Soc. Jpn.* **2003**, *76*, 1783−1792.
(32) Ikegami, M.; Arai, T. Photochromic and Fluorescence Properties of a Hemiindigo in the Presence of Bovine Serum Albumin. *Chem. Lett.* **2005**, *34*, 492−493.
(33) Bobrovsky, A.; Pakhomov, A.; Ponomarenko, S.; Boiko, N.; Shibaev, V. Strong Influence of Generation Number on the Kinetics of Z/E Isomerization in Carbosilane Dendrimers With Azobenzene Terminal Groups. *Polym. Prepr.* **2002**, *43*, 93−94.
(34) Le Bras, L.; Adamo, C.; Perrier, A. Modeling the Modulation of Emission Behavior in E/Z Isomers of Dipyrrolyldiphenylethene: From Molecules to Nanoaggregates. *J. Phys. Chem. C* **2017**, *121*, 25603−25616.
(35) Skinner, P. J.; Cherrier, M. C.; Webb, P. J.; Sage, C. R.; Dang, H. T.; Pride, C. C.; Chen, R.; Tamura, S. Y.; Richman, J. G.; Connolly, D. T.; Semple, G. 3-Nitro-4-amino benzoic acids and 6-amino nicotinic acids are highly selective agonists of GPR109b. *Bioorg. Med. Chem. Lett.* **2007**, *17*, 6619−6622.
(36) Albrecht, B. K.; Audia, J. E.; Gagnon, A.; Harmange, J. C.; Nasveschuk, C. G. *Preparation of tetramethylpiperidinylbenzamide derivatives for use as EZH2 activity inhibitors*. International Patent WO 2012068589A2, 2012.
(37) Alexander, B.; Kumar, S.; Rao, K.; Bala, P.; Bharathiraja, A.; Hariharasubramanian, A.; Girish, A. R.; Srinivas, T.; Ganesh, P.; Hosahalli, S. *Preparation of piperidine derivatives and analogs for use as stearoyl-CoA desaturase inhibitors*. International Patent WO 2009117676A2, 2009.
(38) Cheruiyot, S. K.; Rozners, E. Fluorescent 2-Aminopyridine Nucleobases for Triplex-Forming Peptide Nucleic Acids. *ChemBioChem* **2016**, *17*, 1558−1562.
(39) Sarma, B.; Nath, N. K.; Bhogala, B. R.; Nangia, A. Synthon Competition and Cooperation in Molecular Salts of Hydroxybenzoic Acids and Aminopyridines. *Cryst. Growth Des.* **2009**, *9*, 1546−1557.
(40) Matczak-Jon, E.; Ślepokura, K.; Kurzak, B. X-ray evidence for the relationship between pyridyl side chain basicity and the Z/E preferences of 5-halogen substituted (pyridin-2-yl)aminomethane-1,1-diphosphonic acids; implications for metal ions coordination in solution. *ARKIVOC* **2012**, *4*, 167−185.
(41) Videnova-Adrabinska, V.; Nowak, A.; Janczak, J. Packing similarities and synthon variabilities in aminopyridinium sulfoisophthalates. *Cryst. Growth Des.* **2016**, *16*, 4247−4262.
(42) Aakeröy, C. B.; Schultheiss, N.; Desper, J.; Moore, C. Balancing Hydrogen-Bond Donors and Acceptors in a Family of Bifunctional Aromatic N-Heterocycles. *Cryst. Growth Des.* **2007**, *7*, 2324−2331.
(43) Liu, Z.; Liu, Y.; Li, J.; Zhu, W. Prediction of supramolecular synthons and crystal packings of supramolecular HMX/solvent assemblies. *RSC Adv.* **2017**, *7*, 55482−55488.
(44) Day, G. M. Advances in crystal structure prediction and applications to pharmaceutical materials. *Comput. Pharm. Solid State Chem.* **2017**, *13*, 5163−5171.
(45) Iuzzolino, L.; Reilly, A. M.; McCabe, P.; Price, S. L. Use of Crystal Structure Informatics for Defining the Conformational Space Needed for Predicting Crystal Structures of Pharmaceutical Molecules. *J. Chem. Theory Comput.* **2017**, *13*, 5163−5171.
(46) Oganov, A. R.; Zahed, S. A. *Computer-implemented crystal structure search method*. PCT International Application WO 2018009090A1, 2018.
(47) Long, S.; Parkin, S.; Siegler, M. A.; Cammers, A.; Li, T. Polymorphism and Phase Behaviors of 2-(Phenylamino)nicotinic Acid. *Cryst. Growth Des.* **2008**, *8*, 4006−4013.
(48) Long, S.; Mao, T.; Chen, P.; Liu, M.; Parkin, S.; Zhang, M.; Li, T.; Zhou, P.; Yu, F. Strong Hydrogen Bond Leads to a Fifth Crystalline Form and Polymorphism of Clonixin. *ChemistrySelect* **2017**, *2*, 4942−4950.
(49) Long, S.; Zhou, P.; Theiss, K. L.; Siegler, M. A.; Li, T. Solid-State Identity of 2-Hydroxynicotinic Acid and Its Polymorphism. *CrystEngComm* **2015**, *17*, 5195−5205.
(50) Long, S.; Zhou, P.; Parkin, S.; Li, T. Polymorphism and Solid-to-Solid Phase Transitions of a Simple Organic Molecule, 3-Chloroisonicotinic Acid. *CrystEngComm* **2015**, *17*, 2389−2397.
(51) Chen, P.; Jin, Y.; Zhou, P.; Parkin, S.; Zhang, Z.; Long, S. Solid-State Characterization of 2-[(2,6-Dichlorophenyl)amino]-Benzaldehyde: An Experimental and Theoretical Investigation. *J. Chin. Chem. Soc.* **2017**, *64*, 531−538.
(52) Bernstein, J.; Davis, R. E.; Shimoni, L.; Chang, N. L. Muster aus H-Brucken: ihre Funktionalitat und ihre graphentheoretische Analyse in Kristallen. *Angew. Chem.* **1995**, *107*, 1689−1708.
(53) Etter, M. C.; Macdonald, J. C.; Bernstein, J. Graph-set Analysis of Hydrogen Bond Patterns. *Acta Crystallogr., Sect. B: Struct. Sci.* **1990**, *46*, 256−262.
(54) Etter, M. C. Encoding and Decoding Hydrogen-Bond Patterns of Organic Compounds. *Acc. Chem. Res.* **1990**, *23*, 120−126.
(55) John, A. D. *Lange's Handbook of Chemistry*, 15th ed.; McGraw-Hill Inc., 1998.
(56) Becke, A. D. Density-functional thermochemistry. III. The role of exact exchange. *J. Chem. Phys.* **1993**, *98*, 5648−5652.
(57) Krishnan, R.; Binkley, J. S.; Seeger, R.; Pople, J. A. Self-consistent molecular orbital methods. XX. A basis set for correlated wave functions. *J. Chem. Phys.* **1980**, *72*, 650−654.
(58) Zhao, Y.; Truhlar, D. G. The M06 suite of density functionals for main group thermochemistry, thermochemical kinetics, noncovalent interactions, excited states, and transition elements: two new functionals and systematic testing of four M06-class functionals and 12 other functionals. *Theor. Chem. Acc.* **2008**, *120*, 215−241.
(59) Weigend, F.; Ahlrichs, R. Balanced basis sets of split valence, triple zeta valence and quadruple zeta valence quality for H to Rn: Design and assessment of accuracy. *Phys. Chem. Chem. Phys.* **2005**, *7*, 3297−3305.
(60) Frisch, M. J.; Trucks, G. W.; Schlegel, H. B.; Scuseria, G. E.; Robb, M. A.; Cheeseman, J. R.; Scalmani, G.; Barone, V.; Petersson, G. A.; Nakatsuji, H.; Li, X.; Caricato, M.; Marenich, A. V.; Bloino, J.; Janesko, B. G.; Gomperts, R.; Mennucci, B.; Hratchian, H. P.; Ortiz, J. V.; Izmaylov, A. F.; Sonnenberg, J. L.; Williams-Young, D.; Ding, F.; Lipparini, F.; Egidi, F.; Goings, J.; Peng, B.; Petrone, A.; Henderson, T.; Ranasinghe, D.; Zakrzewski, V. G.; Gao, J.; Rega, N.; Zheng, G.; Liang, W.; Hada, M.; Ehara, M.; Toyota, K.; Fukuda, R.; Hasegawa, J.; Ishida, M.; Nakajima, T.; Honda, Y.; Kitao, O.; Nakai, H.; Vreven, T.; Throssell, K.; Montgomery, J. A., Jr.; Peralta, J. E.; Ogliaro, F.; Bearpark, M. J.; Heyd, J. J.; Brothers, E. N.; Kudin, K. N.; Staroverov, V. N.; Keith, T. A.; Kobayashi, R.; Normand, J.; Raghavachari, K.; Rendell, A. P.; Burant, J. C.; Iyengar, S. S.; Tomasi, J.; Cossi, M.; Millam, J. M.; Klene, M.; Adamo, C.; Cammi, R.; Ochterski, J. W.; Martin, R. L.; Morokuma, K.; Farkas, O.; Foresman, J. B.; Fox, D. J. *Gaussian 16*, Revision A 03; Gaussian, Inc.: Wallingford, CT, 2016.
(61) Grimme, S.; Antony, J.; Ehrlich, S.; Krieg, H. A consistent and accurate ab intio parameterization of density functional dispersion correction (DFT-D) for the 94 elements H-Pu. *J. Chem. Phys.* **2010**, *132*, 154014.
(62) Grimme, S.; Ehrlich, S.; Goerigk, L. Effect of the damping function in dispersion corrected density functional theory. *J. Comput. Chem.* **2011**, *32*, 1456−1465.
(63) Sterling, T. L.; Salmon, J.; Becker, D. J.; Savarese, D. F. *How to build a Beowulf*; MIT Press; 1999.
(64) Pflug, A.; Szyszka, B.; Niemann, J. Simulation of Reactive Sputtering Kinetics in Real In-line Processing Chambers. *Thin Solid Films* **2003**, *442*, 21−26.
(65) Lee, M. L.; Aliagas, I.; Feng, J. A.; Gabriel, T.; O'Donnell, T. J.; Sellers, B. D.; Wiswedel, B.; Gobbi, A. Chemalot and Chemalot

DOI: 10.1021/acs.cgd.8b00840
Cryst. Growth Des. 2018, 18, 4849−4859

Knime: Command Line Programs As Workflow Tools For Drug Discovery. *J. Cheminf.* **2017**, *9*, 1−38.

DOI: 10.1021/acs.cgd.8b00840
Cryst. Growth Des. 2018, 18, 4849−4859